Optimisation of an image plate system with respect to tube voltage

An observer performance study based on chest and pelvis images

David Sjöström

Department of Radiation Physics, Malmö
Lund University

ABSTRACT

In this study we evaluate the clinical image quality of a computed radiography system for different tube voltages. Images of anthropomorphic phantoms were produced and the quality of the images was evaluated using visual grading analysis (VGA) by a group of experienced radiologists. Two different X-ray examinations were investigated: chest PA and pelvis AP. The exposure conditions were set so that the effective dose for each technique was approximately the same in all exposures regardless of the tube voltage. The aim of the study was to investigate if any kV setting was assessed as preferable. Our results show that the image quality is improved when lowering the kV settings in both pelvis and chest radiography with the Fuji computed radiography system used. The improvement is marginal in chest radiography but more pronounced for pelvis investigations. The study also illustrates the differences in effective dose obtained using different methods for calculation.

INTRODUCTION

Optimisation in diagnostic radiology refers to the obtaining of an image quality that satisfies the diagnostic requirements for making a correct diagnosis at the lowest possible patient exposure. To justify the use of ionising radiation in medical diagnosis the stochastic risk of cancer induction and genetic injury must be as low as possible. To be able to express this risk the Internal Commission of Radiation Protection (*ICRP 1990*) have defined the quantity "effective dose". The effective dose is an organ-weighted measure that permits estimates of the risk of partial body radiation exposure to be compared directly to the risk of whole body radiation. Since image quality is relative to the diagnostic requirements there is no exact straightforward definition of this quantity. Internal Commission on Radiation Units and Measurements (*ICRU 1996*) present a wide spectrum of different methods to assess image quality. Some are objective measurements of the system's physical characteristics, e.g. noise and spatial resolution, but ICRU stresses that the human observer should be taken into consideration in the evaluation process.

The method mostly accepted to assess the image quality, incorporating the human observer, is the Receiver Operating Characteristics method (ROC) (*Månsson 1994, ICRU 1996*). The ROC is often referred to as the "golden standard" in evaluation of image quality. ROC is the observer performance method recommended by *ICRU (1996)*. The prerequisite in all ROC analysis is that the true state of each case must be known (i.e. the presence or absence of a signal). Since ROC methods are very time consuming, both in the set-up and the execution of the study, other observer performance methods have been developed. One method is the visual grading analysis (VGA) where the whole image, or parts of the image, is evaluated visually described previously by e.g. *Månsson (1994)* and *Tingberg (2000)*. A specific use of VGA is to compare the visibility of defined anatomical structures with the same structures in a reference image. This provides VGA with an advantage over ROC analysis, where the signal state must be known. VGA, using reference images, is an efficient method when relatively small numbers of radiographs and observations are needed to obtain statistically significant differences between different techniques (*Sund et al. 2000, Tingberg et al. 2000*). The drawback is that, even though the differences in image quality between techniques can be established, it can be hard to predict if this is of diagnostic importance. This is important since the whole idea behind VGA is that the visibility of normal anatomy is believed to describe the ability of the system to reproduce pathological conditions. Therefore studies have carried out where correlations between ROC and VGA have been found (*Sund et al. 2000, Tingberg et al. 2000*).

The optimal use of ionising radiation involves the interplay of three important aspects: the diagnostic quality of the radiographic image, the radiation dose to the patient and the choice of radiographic technique. In 1996 the *European Commission (1996)* published guidelines on all three of these aspects for six routine examinations (chest, skull, lumbar spine, pelvis, urinary tract and breast). Criteria for the radiation dose to the patient are expressed in terms of a reference dose value. The image quality criteria are those considered to be necessary to produce an image of standard quality. The radiographic technique recommendations present examples of techniques where the criteria for radiation dose and image quality are fulfilled. These guidelines do not claim to give strict instructions but can be used as a basis for further development by the radiological community. Recently several investigations have used the criteria

presented in European Commission as a base to select relevant structures for VGA studies (e.g. *Sund et al. 2000, Tingberg 2000 and Tingberg et al. 2000*).

Today, many radiology departments replace their film-screen systems with digital systems. In general, the techniques that have been found appropriate for the film-screen system are also used for the digital system. For chest exposures high kV techniques (125 kV) are customarily used as recommended by the *European Commission (1996).* For pelvis examinations the *European Commission (1996)* recommends a kV setting between 75 kV and 90 kV. Film-based receptors are limited by the fact that a minimum dose is required to achieve an appreciable blackening of the film. The optical density, controlled by the exposure and the film characteristic (i.e. the dynamic range and the film gradient), is therefore crucial for the image quality in a film-screen system. Digital radiography systems, as opposed to film-based systems, are not limited to a narrow dynamic range. With digital processing such as "windowing" e.g. the contrast enhancement factor can be changed and thus low contrast objects not visible on a photographic film can be perceived in a digital image *(Harrison 1988)*. Hence, the optical density level is no longer critical in a digital system and the quality of the image is instead primarily determined by the signal to noise ratio (SNR). Furthermore, the digital receptors are made of different materials to conventional receptors. For instance, the image plate in a CR system consists of a BaF composition with a K-edge (about 40 keV) below the corresponding K-edge for a film-screen system (about 50 keV for gadolinium-based screens) *(Yaffe and Rowlands 1997)*. The mentioned factors contribute to a situation where techniques optimal for screen-film may not necessarily be optimal for digital systems.

Launders et al. (2001) showed that the image quality in chest radiography was improved when decreasing the tube voltage for a digital system (Philips Thoravision system based on an amorphous selenium detector). The study was based on both physical measurements and observations of clinical images.

Physical measurements *(Chotas et al. 1993)* and Monte Carlo simulations *(Sandborg et al. 1994)* have indicated the same phenomena for chest radiography with CR systems. Furthermore *Dobbins et al. (1992)* included the human observer, and studied the threshold detection performance for chest equivalent exposures with results pointing in the same direction. Since these studies include neither the radiologist nor the clinical images, it is difficult to establish if these findings reflect the perceived clinical image quality.

The present study includes both these factors. The image quality was determined using VGA, while anthropomorphic phantoms were used to imitate pelvis and chest examinations. Using anthropomorphic phantoms is a close simulation of real life examinations without exposing human subjects to radiation. In that way it is an initial attempt to see if previous investigations of the physical parameter SNR *(Sandborg et al. 1994, Chotas et al. 1993)* is valid when human observers assess the image quality.

The aim of the study was to investigate if any kV setting was assessed as preferable when the exposure conditions were set so that the effective dose was approximately equal in all exposures regardless of the tube voltage setting.

MATERIAL AND METHODS

Phantoms and radiography system

In the chest study an anthropomorphic phantom, the RSD Torso Imaging Phantom, was used *(Pearce et al. 1979, ICRU 1992)*. The phantom consists of animal lungs, arterial tree filled with blood substitute, artificial skeleton and anatomically realistic mediastinum and pleural cavities. The size of the torso corresponds to the size of an average North American male (75.5 kg/175 cm). According to *ICRU (1992)* the application of the phantom is for assessment of image quality. Figure 1 shows a PA projection of the phantom.

The phantom used in the pelvis study consists of a human skeleton enclosed with tissue equivalent material. An AP projection of the phantom is shown in Figure 2. Based on the opinion of an experienced radiologist, the phantom was regarded as sufficient for assessment of image quality *(Jack Besjakov, Department of diagnostic radiology, Malmö university hospital, Sweden, personal communication, 2001*).

The digital radiography imaging system used in this investigation was a Fuji Computer Radiography system (FCR AC-3 CS/ID) and all images were produced on Fuji's 36 cm x 43 cm imaging plates (Fujifilm Medical systems, Stamford, Connecticut, USA). A brief description of the CR system is presented in Appendix A.

The study was conducted at the department of diagnostic radiology at the hospital of Ystad, Sweden.

Conversion coefficients for matched exposure risk

In this study the effective dose was calculated using conversion coefficients between dose area product (DAP) and effective dose for various exposure parameters, published by the National Radiological Protection Board *(NRPB 1994)*. The NRPB conversion coefficients only cover the range 50 – 120 kVp and 2 – 5 mm Al. To get the conversion coefficients for the beam qualities used in this study the NRPB data had to be extrapolated. To obtain the conversion coefficients a simple logarithmic regression curve was adjusted to the NRPB conversion coefficients. This was done both as a function of filtration and as a function of kV. The fit of the logarithmic curves all matched the NRPB data very closely (r^2>0.99). The conversion coefficient for the desired beam qualities was then extrapolated from the functions of the logarithmic regression (see Table 1).

Table 1. Conversion coefficients for the kV settings used in the study. According to *NRPB (1994)*, the uncertainty for all the conversion coefficients lie below 2 %, and the quoted uncertainty defines an interval having a level of confidence of 95 %. Therefore the standard uncertainty of all conversion coefficients presented in the table is approximately 1 % (2 ÷ 1.96). (The factor for the normal distribution for the 95 % level of confidence is 1.96 *(ISO 1995)).*

Chest PA [7 mmAl]		Pelvis AP [6 mmAl]	
KV	**Conversion factor [mSv/Gycm^2]**	**KV**	**Conversion factor [mSv/Gycm^2]**
70	0.163	50	0.194
81	0.187	60	0.233
90	0.205	63	0.243
102	0.225	66	0.253
109	0.236	70	0.266
117	0.248	73	0.275
125	0.259	77	0.286
130	0.270	81	0.297
140	0.279	90	0.320
150	0.290	102	0.347

Exposure conditions for matched exposure risk

The mAs value used to yield the same effective dose at each kV in both the pelvis and chest examinations was determined as follows: First, the chest phantom and the pelvis phantom were positioned according to the standard exposure conditions at the department of diagnostic radiology at the hospital of Ystad (Table 2).

Table 2. Standard exposure conditions at the department of diagnostic radiology at the hospital of Ystad.

Standard exposure	Pelvis AP	Chest PA
kV setting	70	125
mAs setting	28	6.3
Focus to detector distance (cm)	120	155
Filtration (mmAl)	6	7

Secondly, the kerma area product (KAP) in both standard conditions was measured by using a transmission ionisation chamber (Doseguard 100, RTI Electronics AB, Mölndal, Sweden). The KAP values is assumed to be approximately the same as the DAP-value in the energy range of interest. This is due to the small range of secondary electrons produced in the air cavity. By using the KAP value for these reference exposures and the conversion factors presented in Table 1, the effective dose in both reference conditions were calculated. Using conversion factors for other kV settings the desired KAP values that would yield the same effective dose as the standard exposure were calculated. Because of the discrete steps in the generator setting of the mAs, a precise match to the reference effective dose could not be achieved. Instead the closest mAs settings that resulted in an effective dose below or just above the reference effective dose were used.

The desired and actual KAP values and mAs settings used at each kV for the chest examination are shown in Table 3 together with the resulting effective dose for the actual exposure. The corresponding information for the pelvis examination is presented in Table 4.

Table 3. The table shows the desired and actual KAP values and mAs settings used at each kV for the chest PA. The effective dose calculated from the conversion coefficients in Table 1for the actual exposure is presented in the right column. The standard setting is written in bold text. The relative standard uncertainty of all KAP measurements (estimated by repeating the exposures) was less than 0.4 % for all settings. The uncertainty of the conversion coefficients were presented in table 1. Hence, the combined standard uncertainty of the estimate of the effective dose is less than 1.1 % (1.022+0.42)1/2. The number following the symbol ± is the round off numerical value of the combined uncertainty.

kV	Desired KAP value [mGycm^2]	Tube current x exposure time [mAs]	Measured KAP value [mGycm^2]	Effective dose [μSv]
70	126.5	32	116.2	18.9 ± 0.2
81	110.2	22	109.6	20.5 ± 0.2
90	100.6	14	91.2	18.7 ± 0.2
102	91.6	10	85.9	19.3 ± 0.2
109	87.4	9	85.4	20.2 ± 0.2
117	83.1	7	77.7	19.3 ± 0.2
125	**79.6**	**6.3**	**79.6**	**20.6** ± 0.2
130	76.4	5	73.6	19.9 ± 0.2
140	73.9	4.5	73.2	20.4 ± 0.2
150	71.1	4	75.9	22.0 ± 0.2

Table 4. The table shows the desired and actual KAP values and mAs settings used at each kV for the pelvis AP. The effective dose calculated from the conversion coefficients in Table 1 for the actual exposure is presented in the right column. The standard setting is written in bold text. The relative standard uncertainty (estimated by repeating the exposures) was less than 0.2 % for all settings. The uncertainty of the conversion coefficients were presented in table 1. Hence, the combined standard uncertainty of the estimate of the effective dose is less than 1.04 % $(1.02^2+0.2^2)^{1/2}$. The number following the symbol ± is the round off numerical value of the combined uncertainty.

KV	Desired KAP value [mGycm^2]	Tube current x exposure time [mAs]	Measured KAP value [mGycm^2]	Effective dose [μSv]
50	1399	112	1374	267 ± 3
60	1164	50	1146	267 ± 3
63	1117	40	1078	262 ± 3
66	1072	32	1005	254 ± 3
70	**1020**	**28**	**1020**	**271** ± 3
73	987	25	988	272 ± 3
77	949	20	933	267 ± 3
81	914	16	849	262 ± 3
90	848	12	851	272 ± 3
102	782	8	783	272 ± 3

Image acquisition

Images of the chest and the pelvis phantoms were taken with the kV settings and the mAs settings presented in Table 3 and Table 4, respectively. To minimize differences in the read-out, the phantom was kept in exactly the same position for all exposures. The same image plate (IP), positioned in exactly the same way, was used in each exposure. This was done to eliminate possible differences that could have occurred if different image plates had been used or if the image plate had been rotated between exposures. The exposed image plates were read-out using standard processing alternatives employed clinically for the two types of examinations. Using standard processing the system automatically adjust the raw data to a proper image i.e. the system is working in auto mode (see Appendix A, Figure 10).

Image criteria used for the VGA-study

The evaluation of the chest images was based on a revised version *(Sund et al. 2000, Tingberg et al. 2000, Tingberg 2000)* of the European Image Criteria *(European Commission 1996)*. The image criteria used in this study (Table 5 and Figure 1) differ though from the criteria presented in the revised version since one criterion (no. 7) had to be excluded due to the absence of the corresponding anatomical structure (the carina with main bronchi) in the phantom. The structures that were used in the VGA study were extracted from the criteria.

Table 5. Image criteria for the chest images (cf. Figure 1).

	Image criteria
1	Sharp visualisation of the vessels seen 3 cm from the pleural margin
2	Visualisation of the thoracic vertebrae behind the heart
3	Visualisation of the retrocardiac vessels
4	Sharp visualisation of the pleural margin
5	Sharp visualisation of vessels seen en face in the central area
6	Sharp visualisation of the hilar region

The locations of the anatomical structures described in the criteria in Table 5 are shown in Figure 1.

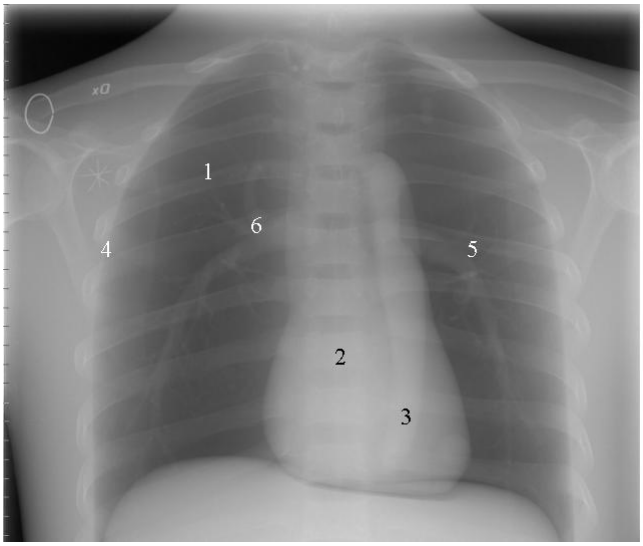

Figure 1. Schematic description of locations of the structures from the image criteria in Table 5

The evaluation of the pelvis images was also based on the European Image Criteria (*European Commission 1996*). These criteria are presented in Table 6.

Table 6. The European Image Criteria for pelvis AP projection (European Commission 1996).

	Image criteria
1	Symmetrical reproduction of the pelvis as judged by the imposition of the symphysis pubis over the midline of the sacrum
2	Visually sharp reproduction of the sacrum and its intervertebral foramina
3	Visually sharp reproduction of the pubic and ishial rami
4	Visually sharp reproduction of the sacroiliac joints
5	Visually sharp reproduction of the necks of the femora which should not be distorted by foreshortening or rotation
6	Visually sharp reproduction of the spongiosa and corticalis, and of the trochanters

From the image criteria in Table 6, a revised version of the image criteria was developed. These criteria are presented in Table 7. The structures that were used in the VGA study were extracted from the criteria.

Table 7. A revised version of the image criteria for the pelvis images (cf. Figure 2)

	Image criteria
1	Visually sharp reproduction of the sacrum (spongiosa)
2	Visually sharp reproduction of the sacral foramina
3	Visually sharp reproduction of pubic and ishial rami
4	Visually sharp reproduction of the the sacroiliac joints
5	Visually sharp reproduction of the femoral neck bilateral

The locations of the anatomical structure described in the criteria in Table 7 are shown in Figure 2.

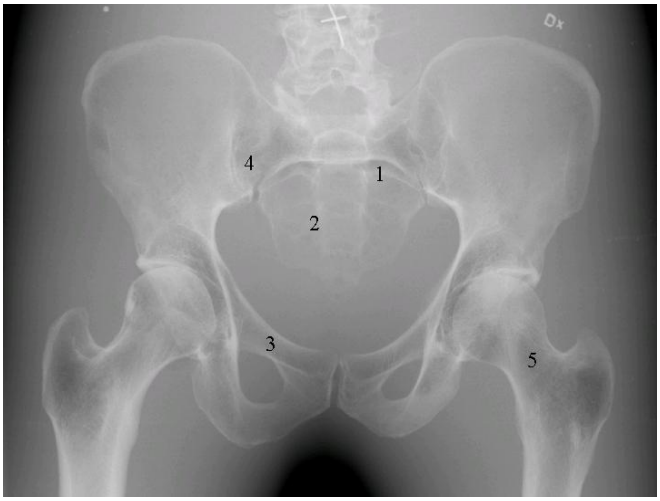

Figure 2. Schematic description of the location of the image criteria in Table 7

The revision was done in collaboration with an experienced, board certified radiologist (*Jack Besjakov, personal communications, 2001*). Some important steps in this process are discussed below.

Criterion 1 and the last part of criterion 5 (Table 6) refer to the positioning of the patient and not to any anatomical landmark and were therefore excluded. The trochanters in criterion 6 (Table 6) and the femoral necks were assumed to be reproduced in the same way in the image and the trochanters were therefore excluded.

Criterion 6 (Table 6) does not specify where cortical and spongiosa bone in the pelvis area should be visually sharply reproduced. According to the radiologist it is the pathology in the sacrum that is most difficult to detect, in a clinical situation. Therefore in criterion 1 (Table 7), which refers to visually sharp reproduction of the sacrum, the importance of also evaluating spongiosa is stressed by stating this specifically in the criterion.

The intervertebral foramina in criterion 2 (Table 6) cannot be seen on an AP projection, and was therefore corrected to sacral foramina resulting in criterion 2 (Table 7).

The observers

Six radiologists participated in the pelvis trial, and five in the chest trial. Five were employed at the hospital and therefore familiar with the equipment and monitors used. One was employed at another hospital but before the study he was trained on the specific equipment and routines used.

The clinical trial

The observers were introduced to the study by a radiologist experienced in the use of the VGA methodology. Each image was assigned a randomly generated code. In this way the observers evaluated the images without any knowledge of the used technique. The images were evaluated on a workstation with two monitors (Siemens SMM 21140P 1.6 k), used for clinical purposes. To simplify the evaluation process the images were sorted in a system showing the reference image on one of the monitors and the image to be evaluated on the other monitor. The reference image was always presented on the same monitor and therefore possible differences in the quality between the monitors don’t influence the results. The images were evaluated by comparing each structure of the image criteria with the structure in the reference image. The radiologists were instructed to observe the images, as they would do in a clinical situation so that the images were displayed in the best possible way. Therefore they were told to change the window settings and they were also allowed to zoom the structures of interest.

Evaluation of clinical image quality

The clinical image quality was evaluated with VGA using a relative rating scale (Table 8).

Table 8. Relative rating scale for VGA

Relative rating	Meaning
	The structure in the image is
-2	Clearly inferior than
-1	Slightly inferior than
0	Equal to
+1	Slightly better than
+2	Clearly better than
	the structures in the refererence image

A mean score, the visual grading analysis score (VGAS) for a group of images taken with the same radiographic technique, can be calculated with the following equation (Tingberg 2000):

$$VGAS = \frac{\sum_{i=1}^{I}\sum_{s=1}^{S}\sum_{o=1}^{O} G_{i,s,o}}{I \cdot S \cdot O}$$

where,

$G_{i,s,o}$ = Grading (-2,-1,0,+1 or +2) for image i, structure s and observer o
I = Number of images per technique
S = Number of structures
O = Number of observers

The result for the individual observer is denoted $VGAS_o$.

In this study nine images were evaluated (i.e. compared with the reference image) for each examination. Each image was taken with a different technique and therefore the number of images per technique, I (for both the pelvis and the chest study), is equal to one. For the pelvis the number of structures, S, were five, and the corresponding number for the chest were six. Six observers evaluated the images of the pelvis, whereas five observers evaluated the images of the chest.

A comparison between the different VGAS for different techniques, for both chest and pelvis, was performed to evaluate if any tube voltage setting was preferable.

Statistics

The standard uncertainty (one standard deviation) of the VGAS was estimated with the mean score for each observer ($VGAS_o$).

To be able to establish the statistical validity of changes in the VGAS, an analysis of variance (ANOVA) in conjunction with a method for multiple comparisons, the Newman-Keuls (NK) test was performed. This test has been used earlier in VGA studies to establish significant differences (e.g. *Leitz et al 1993, Sund et.al. 2000*). The

statistical analysis was done using Statistica® (Release 5.1) and the null hypothesis tested was that there was no difference between two techniques.

Comparison of the effective dose calculated with three different methods

Several computer programs for estimating the effective dose of an X-ray examination are available, e.g. the software WinODS (RTI Electronics, Mölndal, Sweden) and the software PCXMC (Stuk, Radiation and nuclear safety authority, Helsingfors, Finland). Both of these methods are based on Monte Carlo calculated conversion coefficients. In WinODS and PCXMC you obtain the effective dose from a specific technique by entering the kerma area product, the patient size, the field size, the focus skin distance etc. (Figure 3). WinODS also gives the opportunity to enter the sex of the patient.

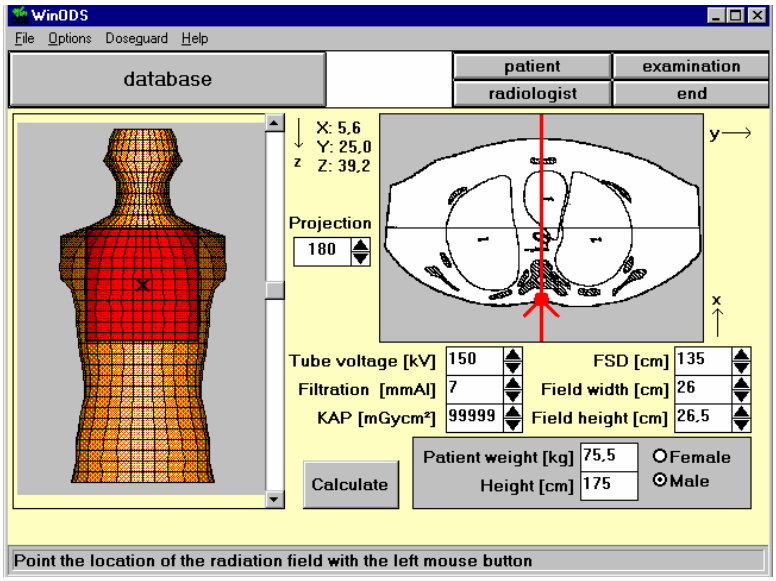

Figure 3. WinODS data input

It is of course of interest to study if the various programs give approximately the same effective dose for all exposures. With WinODS and PCXMC geometrical factors e.g. patient size, field size etc. can be compensated for. The geometrical factors for the chest calculation are shown in Figure 3. This data input form and it's equivalent for the pelvis was used to be able to match the dose calculations with PCXMC to the dose calculations with WinODS. Hence, the field size, field position, focus skin distance etc. were the same for these two calculation methods (Table 9). However it was not possible to compensate for the patient size etc. when using the NRPB data.

Table 9. The exposure conditions used when calculating the effective dose with the three programs. For WinODS and PCXMC the field size refers to the field size at the patient and for NRPB the field size refers to the field size at the detector.

	NRPB		**WinODS**		**PCXMC**	
	Chest PA	**Pelvis AP**	**Chest PA**	**Pelvis AP**	**Chest PA**	**Pelvis AP**
Filtration [mmAl]	7	6	7	6	7	6
FSD [cm]	100	75	135	100	135	100
Field size [cm]	35 x 44	42 x 41	26x26.5	28x19	26x26.5	28x19
Patient Height(cm)/Weight(kg)	-	-	175/75.5	175/75.5	175/75.5	175/75.5
Sex	Herma-phrodite	Herma-phordite	Male and Female	Male and Female	Herma-phrodite	Herma-phordite

The NRPB conversion coefficients for the different techniques are presented in Table 1. By dividing the effective dose with the KAP value, the corresponding conversion coefficients for WinODS and the PCXMC are obtained. There is however no possibility to estimate the uncertainty of the effective dose for these two software. This information is neither given by the manufacture nor presented when calculating the effective dose.

RESULTS

Clinical image quality of the chest images

The results from the evaluation of the quality of the chest images indicate that the VGAS is higher for lower kV settings (Figure 4). The figure shows an increase in VGAS by decreasing kV. The VGAS, range from –0.2 (for the 141 kV setting) to +0.7 (for the 70 kV setting).

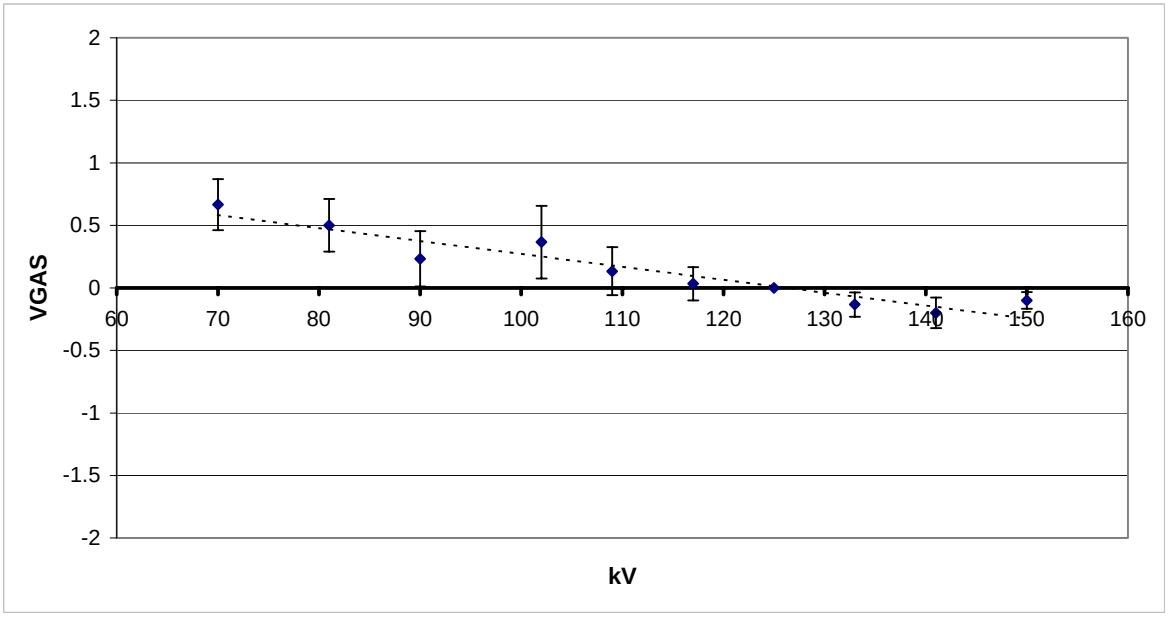

Figure 4. The VGAS for the chest for different kV settings. The bars indicate the statistical uncertainty (one standard deviation). The broken line (r^2=0.899) indicates that there is a linear relationship between VGAS and kV, and also the obvious trend that the VGAS is better for lower kV settings.

The differences in VGAS were not found statistically significant with the NK-test for most of the kV settings. Using the 95 % confidence limit (i.e. $p<0.05$) only one significant difference was found, namely between the 70 kV setting and the 141 kV setting ($p=0.033$). Additionally two combinations show a reasonable statistically significant difference at the 90 % confidence limit (i.e. $p<0.1$). These somewhat less significant differences were found between the 70 kV setting and the 133 kV setting ($p=0.054$) and between the 70 kV setting and the 150 kV setting ($p=0.061$). All other combinations had a $p>0.1$.

Clinical image quality for the pelvis images

The results from the evaluation of the pelvis images indicate that the VGAS is superior for lower kV settings (Figure 5). The figure shows an increase in VGAS by decreasing kV. The VGAS, range from –1 (for the 100 kV setting) to +1.4 (for the 50 kV setting).

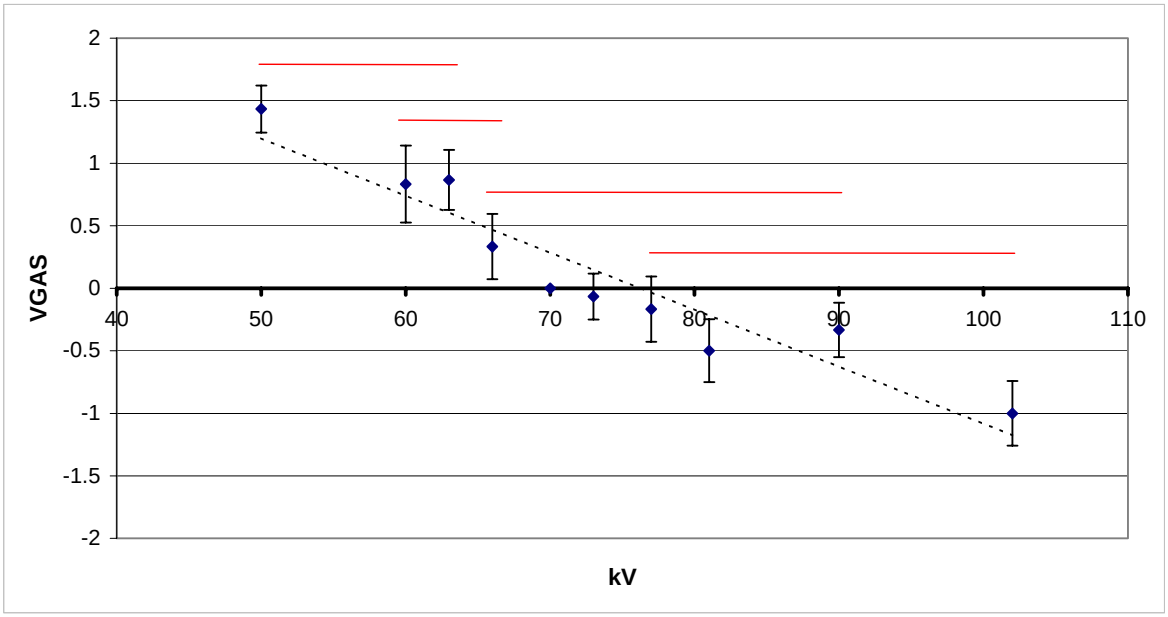

Figure 5. The VGAS for the pelvis for different kV settings. The bars indicate the statistical uncertainty (one standard deviation). The broken line (r^2=0.8975) indicates that there is a linear relationship between VGAS and kV and also the obvious trend that the VGAS is superior for lower kV settings. The horizontal solid lines connecting two tube voltages or more, indicates that no statistical difference between these tube voltages were found with Newman-Keuls test (i.e p>0.05).

In Figure 5 the horizontal solid lines join the kV settings that could not be statistically separated from each other with the NK-test (p>0.05). Small changes in the kV settings could not be statistically separated from each other. However, statistically significant differences (i.e. p<0.05) were found for bigger changes in kV setting e.g. between the lower kV settings (50 kV, 60 kV and 63 kV) and the higher kV settings (70 kV, 73 kV, 81 kV, 90 kV and 102 kV).

Calculation of effective dose

Figure 6 shows the conversion coefficients for the three calculation methods for the chest PA examination.

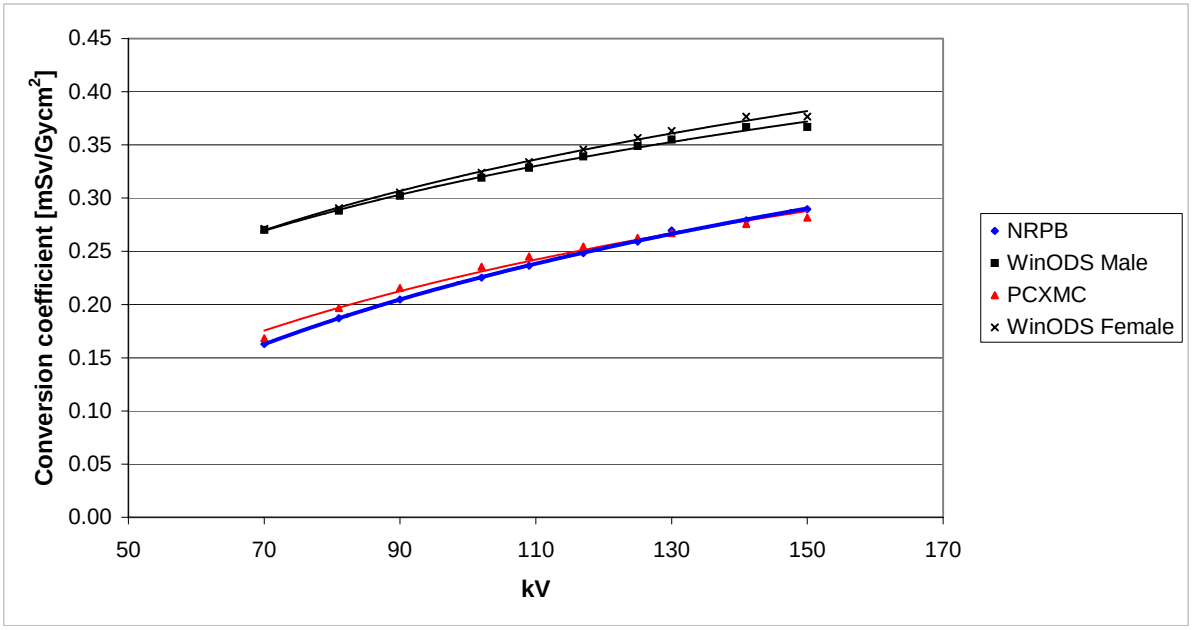

Figure 6. Conversion coefficients for chest PA, calculated with three different methods. The settings were approximately the same for PCXMC and WinODS (c.f. Table 9).

Figure 6 shows that the conversion coefficients for WinODS are approximately 0.1 mSv Gy^{-1} cm^{-2} higher, than for the other two calculation methods. This implies that calculations with WinODS will result in a higher effective dose. The figure also shows that the WinODS conversion coefficient increase with approximately 40 % between 70 and 150 kV, whereas the corresponding increase with NRPB and PCXMC is approximately 80 % and 70 % respectively.

The calculated effective doses for the three different methods, for the measured KAP values (c.f. Table 3), are presented in Table 10.

Table 10. The calculated effective doses, for the actual chest exposures (Table 3), calculated with the three different methods.

kV	Effective dose [µSv] NRPB	Effective dose [µSv] PCXMC	Effective dose [µSv] WinODS Male	Female
70	18.9 ± 0.2	19.6	31.4	31.5
81	20.5 ± 0.2	21.6	31.6	31.8
90	18.7 ± 0.2	19.7	27.5	27.8
102	19.3 ± 0.2	20.2	27.4	27.8
109	20.2 ± 0.2	20.9	28.1	28.5
117	19.3 ± 0.2	19.8	26.3	26.8
125	**20.6** ± 0.2	**20.9**	**27.8**	**28.4**
130	19.9 ± 0.2	19.6	26.1	26.7
140	20.4 ± 0.2	20.2	26.8	27.6
150	22.2 ± 0.2	21.4	27.8	28.6

Table 10 shows that the effective dose for the measured exposures is approximately equal to the reference effective dose within the same calculation method. The calculation with WinODS for the lowest kV settings (70 and 81 kV) and the calculation with NRPB for the highest kV setting (150 kV) are the most evident exceptions.

Calculations with the NRPB and PCXMC methods result in an effective dose between 19 μSv and 22 μSv. The WinODS gave higher effective dose values (28 μSv for the reference exposure).

Figure 7 shows the conversion coefficients for the three calculation methods for the pelvis AP.

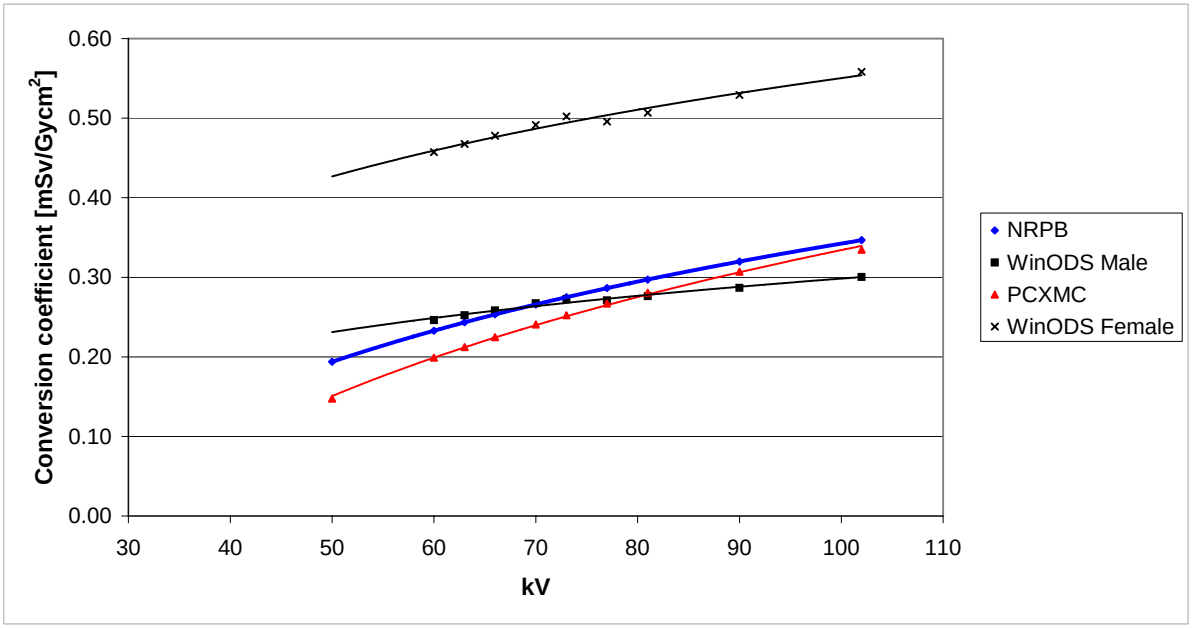

Figure 7. Conversion coefficients for pelvis AP calculated with the three different methods. The settings were approximately the same for WinODS and PCXMC (c.f. Table 9).

The figure shows that there is a big difference in the relation between kV and conversion coefficient for the different calculation methods, in particular when comparing the WinODS method with the other two methods. The calculations with WinODS for female are approximately 85 % higher than calculations for male.

Table 11 shows the calculated effective doses, for the three methods, for the measured KAP values (c.f. Table 4), are presented in Table 11.

Table 11. The calculated effective doses, for the actual pelvis exposures (Table 4), calculated with the three different methods.

kV	Effective dose [μSv] NRPB	Effective dose [μSv] PCXMC	Effective dose [μSv] WinODS	
			Male	Female
50	267 ± 3	203		
60	267 ± 3	228	283	525
63	262 ± 3	229	272	504
66	254 ± 3	226	260	480
70	**271** ± 3	**246**	**273**	**501**
73	272 ± 3	249	269	496
77	267 ± 3	249	253	463
81	262 ± 3	238	234	430
90	272 ± 3	261	244	450
102	272 ± 3	262	235	437

The effective dose for all kV settings calculated with the NRPB method is almost equivalent, which we aimed for. However, calculations with the other two methods showed deviations compared to the reference exposure. The effective doses calculated with WinODS give higher effective dose for the lower kV settings and lower effective dose for the higher kV settings compared to the reference exposure. With the PCXMC the opposite is true i.e. the higher kV settings results in a higher effective dose compared to the reference setting.

DISCUSSION

Our results indicate that the image quality, assessed with VGA, is improved for lower kV settings compared to higher kV settings, in both chest and pelvis examinations (Figure 4 and Figure 5). This was more evident in the pelvis case (Figure 5) than in the chest case (Figure 4). The general trend shows an increase in VGAS by decreasing kV. (Note that the linear regression line only shows the obvious trends i.e. no statement is arisen that the relation between kV and VGAS is truly linear). Even if differences in VGAS only are statistically supported ($p<0.05$) in a few cases, especially in the chest case, the general trends support the conclusion that the image quality is improved when decreasing kV.

Chotas et al. (1993) and *Sandborg et al. (1994)* have studied the physical quantity SNR for situations similar to ours. Our results (Figure 4 and Figure 5) seem to be in accordance with these previous studies.

Chotas et al. (1993) have made measurements of the SNR for chest AP. In their study they evaluated the SNR for different kV settings with a CR-system and the exposure conditions were set so that the effective dose was approximately equal in all exposures. A slight increase in SNR in the lung was found when lowering the tube voltage, whereas the SNR values in two other regions (the mediastinum- and subdiaphragm region) where equivalent for all kV settings. Hence, the change in SNR could be a possible explanation to our slight increase in VGAS when lowering the kV in the chest study (Figure 4).

Sandborg et al. (1994) have performed Monte Carlo simulations for a receptor model representing the Fuji computed radiography system. In their study they calculated how the mean absorbed dose to a homogeneous block shaped phantom, corresponding to an adult chest examination and an adult lumbar spine examination, varies for different kV settings for a constant SNR (equal to five). Assuming that the simulations for the lumbar spine and the chest examinations correspond to our two situations one can make some interesting comparisons. The simulations show that the optimal tube voltage is 70-90 kV for the chest examination and 55-65 kV for the lumbar spine examination. The photon energy spectra used for the simulations corresponds to a total filtration of 3 mm Al. Hence, one can predict that the optimal tube voltage in our study will be slightly lower than what *Sandborg et al.* found, since the higher filtration results in a higher mean energy. These results indicate that the VGAS (Figure 4 and Figure 5) would drop if the tube voltage decreased just below what we used in this study for both examinations. Unfortunately this could not be verified by our study since we did not decrease the kV settings that far as this was supposed to give to long exposure times. Furthermore, the simulations show that mean absorbed dose to the phantom increase more rapidly when the tube voltage is increased in lumbar spine examination compared to the chest examination, which is in accordance with our findings. (The difference in the VGAS in the pelvis case (Figure 5) is more evident than in the chest case (Figure 4)).

These two studies are not identical to ours. Their results reflect a specific task dependent situation whereas our results reflects an overall impression of the clinical image quality. However, the comparison indicates that the assessment of the image quality in our study (Figure 4 and Figure 5) is reflected by the SNR in the observed regions. Since their results, seems to be in accordance with our findings it would be

desirable to perform future studies to investigate any possible correlation between the physical quantity (SNR) and the observer performance method (VGAS). In such a study each criterion must be analysed separately. This is outside the scope of this report. The lack of statistics due to too few images and observers, is another reason why we don't present the criterion separately. In a correlation study a more rigorous observer study is needed. Besides more images and observers it is also desirable to control the viewing conditions (by e.g. printing the images).

The method is founded on that the effective dose is approximately the same for all exposures. In this study we used data published by *NRPB (1994)* to control the exposure conditions. The NRPB data have been used earlier when calculating the effective dose by e.g. Chotas et.al. (1993) and Launders et.al. (2001). With this method the effective dose was close to equivalent to the effective dose for the reference setting, for both examinations (Table 3 and Table 4). In this study we also investigated the calculation of the effective dose with two other methods. In the pelvis case (Figure 7 and Table 11) the differences between the methods is significant between WinODS and the other two methods. It is difficult to identify the main cause for the differences between the methods since this depend on the basics in the Monte Carlo simulations (e.g. voxel sizes in the phantom model). WinODS allows the option to state the patient's sex, which could partly explain the discrepancy to the other two methods in the pelvis area. Assume that we had used WinODS instead of NRPB in the pelvis case. Then the differences in KAP value used (to control the exposure settings) for each kV would be less pronounced. Hence, there is a possibility that the differences in VGAS between high and low kV would be smaller in the pelvis case if we had used the WinODS method. Figure 6 and Table 10 shows that the effective dose is almost the same, irrespective of the calculation method, for the chest exposures. Even if any of the other two methods had been used to control mAs setting in the chest case it would probably result in approximately the same VGAS.

According to the *European Commission (1996)*, the exposure time is recommended to be less than 20 ms for chest examinations and less than 400 ms for pelvis examinations. In examinations of patients it is important to have short exposure times because of the risk that the image will be blurred due to organ and patient motion. These effects did not influence the VGAS in our study since we used phantoms. The longest exposure time in our study, corresponding to the lowest kV settings, was 194 ms for the pelvis and 45 ms for the chest. Tube voltage settings lower than 102 kV resulted in exposure time over 20 ms in the chest study. Therefore it is possible that the observed image quality (VGAS) would decrease for the lower kV settings if real patients were used instead of phantoms. For the pelvis the exposure time is not a problem (according to the guidelines (*European Commission 1996*) even at the lowest tube voltage setting. The use of phantoms can also be criticized since the effect of e.g. different patient sizes is ignored. To be able to determine the influence of anatomical noise (e.g. patient and organ motion) and the size of the patient it is desirable to perform studies with patients.

Our result is an initial indication that the observed image quality is improved, for the same risk to the patient, when lowering the kV in computed radiography of chest and pelvis. Compared with conventional radiography our result is especially remarkable in the chest case, where the guidelines (European Commission 1996) suggest the use of high kV technique.

CONCLUSIONS

Our results indicate that the image quality is improved when lowering the kV setting in both pelvis and chest radiography with FCR. In the chest case the difference in image quality was small between the techniques used (70 – 150 kV) while the difference was more obvious in the pelvis case.

ACKNOWLEDGEMENTS

First of all I would like to thank my supervisor Anders Tingberg for all his support. I would also like to thank Sören Mattsson for additional support, giving me the opportunity to partake in the interesting meeting in Magdeburg, Dec. 2001 and for offering me use his limousine service to and from Malmö.

I would like to thank all the employees at the radiology department at the hospital of Ystad. A special thanks to all the radiologists who participated in this study.

To Jack Besjakov for helping me define the criteria for the study.

To all the other employees and colleagues at the radiophysics department in Malmö, especially Peter Walenius for his skills in radiology and my roommates; Jonas, Helene and Anna for looking out for me.

To the Commission of the European Communities (CEC) for financial support.

And finally, to my parents and my girlfriend for their support.

REFERENCES

Chotas H.G, Floyd C.F, Dobbins 3rd J.T, Ravlin CE. *Digital Chest Radiography with Photostimulable Storage Phosphors*: *Signal-to-Noise Ratio as a Function of Kilovoltage with Matched Exposure Risk*. Radiology 186, 395-398. (1993).

Dobbins 3rd J.T, Rice J.J, Beam C.A, Ravin C.E. *Threshold Perception Performance with Computed and Screen-Film Radiography: Implications for Chest Radiography.* Radiology 183, 179-187. (1992)

European Commission. *European guidelines on quality criteria for diagnostic radiographic images.* EUR 16260, Brussels. (1996)

Harrison R.M. *Digital radiography*. Phys.Med.Biol. 33, 751-784. (1988)

ICRP. *Recommendations of the International Commission on Radiological Protection. ICRP publication 60.* Pergamon Press, Oxford. (1991)

ICRU. *Phantoms and computational models in therapy, diagnosis and protection.* ICRU Report 48. ICRU Publications, Bethesda, MD, USA. (1992)

ICRU. *Medical imaging – The assessment of image quality. ICRU Report 54.* ICRU Publications, Bethesda, MD, USA. (1996)

ISO. *Guide to the expression of uncertainty in measurements.* (1995)

Launders J.H, Cowen A.R, Bury R.F, Hawkridge P. *Towards image quality, beam energy and effective dose optimisation in digital thoracic radiography*. European Radiology 11, 870-875. (2001)

Leitz W.K, Månsson L.G, Hedberg-Vikström B.R.K, Kheddache S. *In search of optimum chest radiography techniques.* The British Journal of Radiology 66, 314-321. (1993)

Månsson L.G. *Evaluation of radiographic procedures. Investigations related to chest imaging. Thesis.* Göteborgs universitet, Göteborg. (1994)

NRPB. Hart D, Jones DG and Wall BF. *Estimation of Effective Dose in Diagnostic Radiology from Entrance Surface Dose and Dose-Area Product measurements.* National Radiological Protection Board. ISBN 085951 3637. (1994)

Pearce J.G, Milne E.N.C, Gillian G.D, Roeck W.W. Development of a radiographic chest phantom with disease simulation. Invest Radiol 14, 181-184. (1979)

Sund P, Herrman C, Tingberg A, Kheddache S, Månsson L.G, Almén A, Mattsson S. *Comparison of two methods for evaluating image quality of chest radiographs*. Proceedings of SPIE Vol. 3981, 251-257. (2000)

Sandborg M, Dance DR, Alm Carlsson G, Persliden J, Tapiovaara MJ. *A Monte Carlo study of grid performance in diagnostic radiology: task-dependent optimisation for digital imaging.* Phys.Med.Biol 39, 1659-1676. (1994).

Tingberg A. *Quantifying the quality of medical X-ray images. An evaluation based on normal anatomy for lumbar spine and chest radiography. Thesis.* Lunds University, Malmö. (2000)

Tingberg A, Herrman C, Besjakov J, Rodenacker K, Almén A, Mattson S. *Evaluation of lumbar spine images with added pathology.* Proceedings of SPIE Vol 3981, 34-42. (2000)

Yaffe M.J, Rowlands J.A. *X-ray detectors for digital radiography*. Phys.Med.Biol 42, 1-39. (1997)

Fuji manuals

Fuji Film Imaging and Information. Chapter 3 (1996)
Fuji Film Imaging and Information. Chapter 4 (1996)
Fuji Film Technical Review No. 3. (1993)

Appendix A - Brief description of the CR-system

In order to familiarise the reader with the concept of the Fuji CR-system a brief description is presented below. For a more precise and complete description the reader is referred to the Fuji manuals. (Fuji Film Imaging and information Chapter 3 and Chapter 4 (1996), Fuji Film and information Technical Review No.3 (1993)).

After the image plate is exposed by X-rays, it is read in an image reader. By stimulating the image plate with laser, visible light is emitted and detected by a photomultiplier tube. The intensity of the emitted light is proportional to the intensity of the exposure. The first quadrant (Figure 8) shows the relationship between the stimulated luminiscent intensity and the incident X-ray dose. However, an immediate digitisation of the information captured on the image plate (IP) would, because of its wide exposure range, result in an image with poor density resolution. As a consequence of this the system uses what they call an Exposure Data Recogniser (EDR).

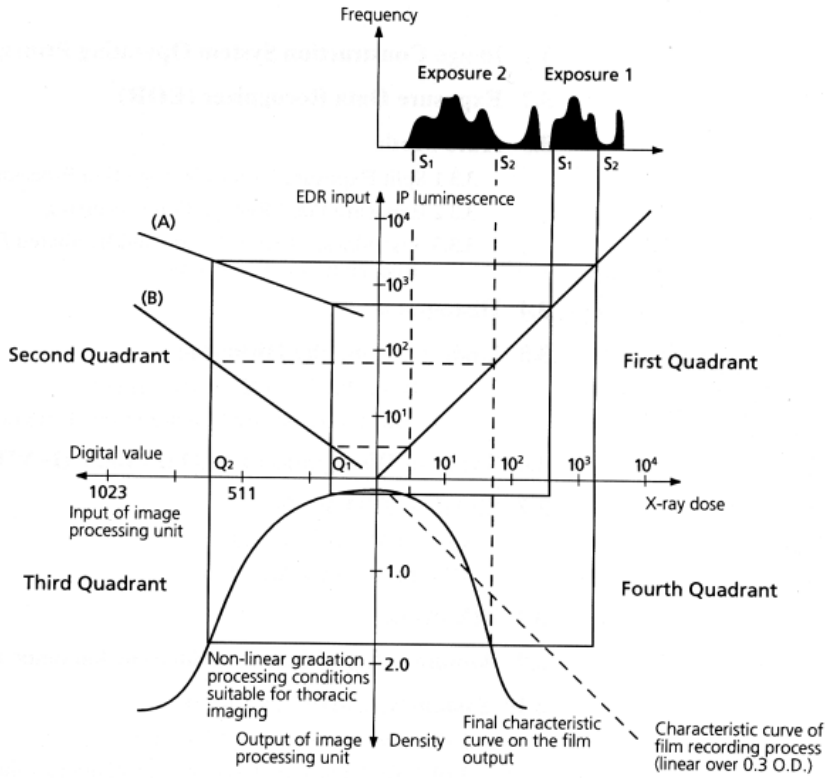

Figure 8. Principles of operation of the FCR system (Fuji Chapter 3 1996).

The second quadrant in Figure 8, illustrates the EDR i.e. the relationship between the input and output signals to and from the image reader. An image data matrix is constructed from the pre-reading of the IP. From this draft matrix the irradiated field is identified and the incident X-ray dose-histogram is determined (Figure 9). The histogram analysis makes it possible to adjust reading conditions, i.e. the gain of the amplifier (determined by the reading latitude L) and the sensitivity of the photomultiplier (determined by the sensitivity S).

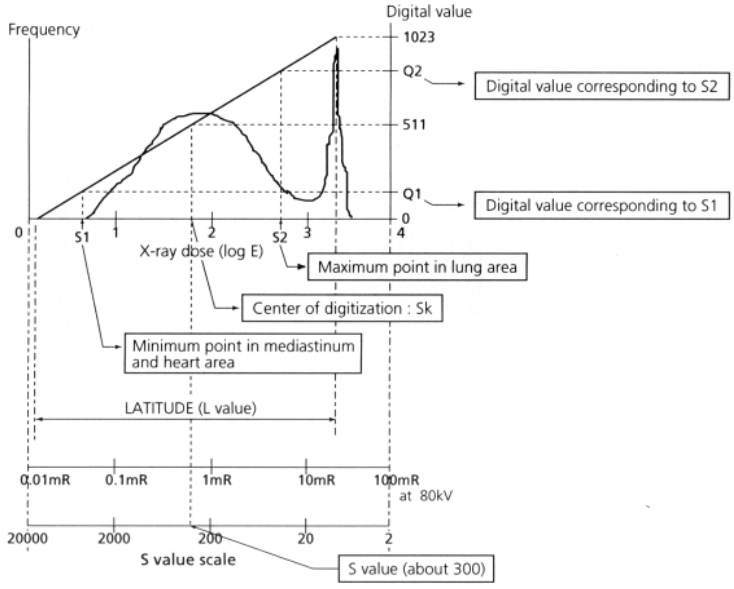

Figure 9. The X-ray dose (photostimulable luminisence intensity) is shown on the horizontal axis and the frequency (number of pixels) of a specific level for each X-ray dose is shown on the vertical axis. The L-value is the X-ray dose range corresponding to digital range 0 to 1023. The S-value is the S scale value corresponding to pixel value 511 (*Fuji Chapter 3 1996*).

Figure 9 shows how the EDR finds the minimum dose (S_1) and the maximum dose (S_2) of an X-ray dose histogram of a chest. From these two points the FCR system assign the density, corresponding to the digital values Q_1 and Q_2. Since the shape of the histogram changes with the anatomical region, the points that determine the reading conditions (S and L) are chosen differently. Hence, EDR provides with different read-out options, suitable for different anatomical regions (Figure 10).

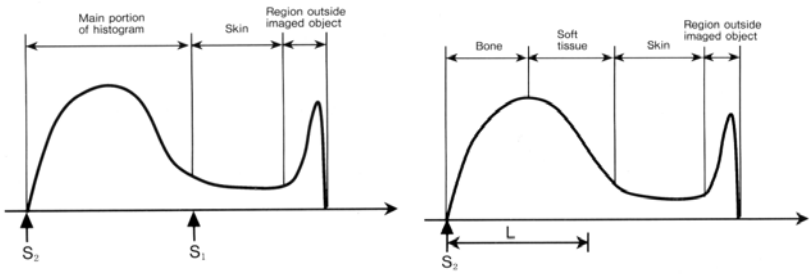

Figure 10. Examples of different alternatives for histogram analysis used in auto-mode . These alternatives are suitable for different anatomical regions. Auto II – diagnosis of bone to soft tissue e.g. diagnosis of the chest and the pelvis regions (left), and Auto V – diagnosis of bone (right). (*Fuji Computed Radiography Technical Review No.3 1993*).

When sensitivity and latitude are automatically adjusted, as described above, the EDR works in auto-mode. (The EDR can also work in fix mode, where L and S are fixed, and in a semi auto mode, where L is fixed but S is automatically adjusted).

In Figure 9 it is shown that an increase in absorbed dose to the detector results in a decrease of the S-value. When the tube voltage is increased the dose histogram will change due to the difference in absorption. In that way higher energy result in smaller dynamic range (i.e. smaller L-value). A general assumption is that the L value is

determined by the kV setting and the S value is determined by the mAs setting (*personal communication, Peter Lazaraz, Fuji, Sweden, 2001*).

When the digitisation is completed, the image can be enhanced with gradation processing (controls the contrast), and spatial frequency processing (controls the sharpness). These processing alternatives are pre-determined by the system. The third quadrant in Figure 8 shows an example of a gradation curve suitable for chest diagnosis. Figure 11 shows other pre-determined gradation curves available in the CR-system.

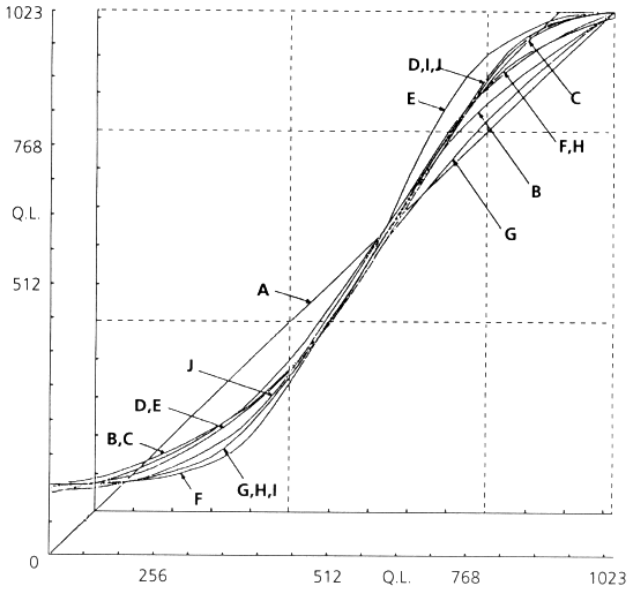

Figure 11. Examples of different gradation curves in the CR-system. (Chapter 4 1996).

The images processed with the CR can be printed on film. The fourth quadrant in Figure 8 illustrates the final characteristic curve for the film output.